International Journal of Metallurgical &
Materials Science and Engineering (IJMMSE)
ISSN(P): 2278-2516; ISSN(E): 2278-2524
Vol. 6, Issue 1, Feb 2015, 35-56

TRANS STELLAR
•Journal Publications •Research Consultancy

EFFECT OF METALLURGICAL PARAMETERS ON THE PERFORMANCE OF AL-CU BASED ALLOYS

G. A. ZAKI[1], A.M. SAMUEL[2], H.W. DOTY[3]& F.H. SAMUEL[4]

[1,4]Université du Québec à Chicoutimi, Québec, Canada

[2,3]General Motors, Department ofMaterials Engineering, Pontiac, MI, USA

ABSTRACT

The present study was performed on a new Al-Cu alloy, designed for automotive applications. This alloy contains Al-2%Cu-1.32%Si-0.42%Mg-0.58%Fe-0.59%Mn-0.07%Ti. All samples were obtained using low pressure die casting technique. For comparison, another set of samplease were produced applying gravity die casting method. It was determined that the alloy containing (0.5% Zr + 0.15% Ti) was the most effective in maximizing the alloy tensile strength over the range of aging temperatures, from 155°C to 300°C. The addition of Ag is beneficial at high aging temperatures, in the range of 240°C-300°C when added simultaneously with 0.27 wt% Zr. However, it is less effective when compared to high Zr concentration (about 0.62 wt%) at the same levels of Ti. It is concluded that the alloy tensile properties may determined by contributions of different strengthening mechanisms mainly the grain size, the volume fraction of intermetallics produced, and evolution and growth of the hardening precipitates with respect to the aging conditions.Quality charts constructed from tensile properties data may be used for the selection of the appropriate metallurgical conditions for tailoring the alloy properties to those required for a specific application. Increasing the copper content from 2wt% to 3.5 wt% does not produce significant increase in the alloy strength.

KEYWORDS: Aluminum Alloys, Heat Treatment, Casting Technology, Tensile Properties, Grain Structure

Received: Nov15, 2015; **Accepted:** Dec 19, 2015; **Published:** Jan 05, 2016; **Paper Id.:** IJMMSEFEB20163

Original Article

INTRODUCTION

Among the many techniques which exist for casting alloys, three main techniques are used for casting aluminum alloys: (1) sand casting, (2) permanent mold casting and (3) pressure die casting. Chu et al. [1], Makhloufet al. [2], and Street [3] reported that while all three techniques have been extensively used in the production of diverse aluminum castings, the die casting technique provide near-net-shape product. Also, die casting is a rapidly repetitive operation in which identical parts are cast at high production rates. Similar recommendation has been made by Elgallad et al. [4].

In the past 15 years, the TAMLA research group (at the Université du Québec à Chicoutimi) worked to develop a new alloy for automotive applications. Based on the results reported by several authors [5-9], this alloy, temporary coded alloy 220, was selected for study based on its promising potential for use in automotive applications. Alloy 220A has a composition consisting of Al-2 wt%%Cu-1.32 wt%%Si-0.42 wt%%Mg-0.58 wt%%Fe-0.59 wt%%Mn-0.07 wt%%Ti. The 220 alloy containsa very low amount of silicon that enough to tie-up the iron in the form of α-Al_{15}(Fe, Mn)$_3Si_2$. The amount of copper in the base alloy was kept at 2% compared to 3.5 wt% in the 319 alloy which is widely used in the automotive industries [10]. In another study, Pucellaet al. [11] reported on the effect of Sr addition in altering the precipitation order of the α-Al_{15} intermetallic from post α-Al

dendritic to pre-dendritic precipitation which leads to strengthening the soft α-Al matrix and hence better mechanical properties.

According to Nabawy et.al. [12], the refinement of the grain structure obtained with the Zr-Ti or Ti additions decreased the hot-tearing severity as result of an increase in the number of intergranular liquid films per unit volume and a delay in reaching the coherency point. Increasing the Si content reduced the hot-tearing susceptibility of the Al-2wt%Cu alloy considerably; this reduction is attributed to an increase in the volume fraction of eutectic in the structure, and a decrease in the freezing range of the alloy. The addition of Sr caused deterioration in the hot-tearing resistance of the base alloy as a result of the formation of Sr-oxides and an extension of the freezing range of the alloy. It was also observed that α-Fe particles may obstruct the propagation of hot-tearing cracks. The 1%wtSi-containing Al-2wt%Cu alloy was judged to be the best composition in view of its low hot-tearing susceptibility.

It was reported by the present authors [13, 14] that Sr could cause fragmentation and dissolution of the brittle platelet-like β-Fe intermetallic phase whose presence is known to cause feeding problems during solidification and result in porosity formation, as well as reduce the mechanical properties [15]. Therefore, an examination of the phases formed in the 220 alloys containing the various additives used in our study will be very helpful in understanding the tensile and hardness properties that were determined for these alloys. Table 3 summarizes the average volume fraction of intermetallics in 220 alloy series in the as cast condition.

The precipitation hardening process in Al-Cu alloys takes place through the sequential formation of precipitates, namely the GP zones (GP1 and GP2) which are coherent with the matrix, followed by the metastable θ″ and the metastable semi-coherent θ′ phases, and finally the non-coherent θ-$CuAl_2$ phase. Hardening accompanies the formation and growth of the GP zones caused by the distortion of the matrix lattice which hinders dislocation movement. According to Voncina et.al. [16] as these precipitates transform successively to θ″ and θ′ phases, the latter contribute to increasing the strengthening level of the alloys, whereas with the precipitation of the θ-$CuAl_2$ phase, the strength begins to decrease due to the lack of coherency between the precipitates and the metal matrix.

Another point to consider is that the 220 base alloy has a complicated chemical composition, added to which the various additives used to prepare the different 220 alloys studied will result in a wide variety of age-hardening phases which will form during aging. Eskin [17] investigated the decomposition of supersaturated solid solution in Al-Cu-Mg-Si alloys. The precipitation sequences in this system may occur either simultaneously or independently.

In the present study, the hardness and tensile properties of the new Al-2wt%%Cu based alloy, were investigated. The base alloy was used to prepare other alloys by adding Sr, Ti, Zr, and Ag to the melt, individually or in different combinations. Castings were made using the low-pressure die casting (LPDC) technique which provides several advantages, among them high productivity and reduced machining costs. In order to emphasize on the tensile properties obtained from the new Al-Cu, a 319 alloy that is widely used in the automotive industryhas been considered [13]. Also, for the purpose of comparison, castings from the 220 alloys were made applying the gravity die casting (GDC) technique.

EXPERIMENTAL PROCEDURE

Samples Preparation

Table 1 shows the chemical composition of the two base alloys i.e. 220 and 319 alloysused in the present work. The calculated average densities of the two alloys are 2.78 and 2.93 g/cm3, respectively. The base alloys were received in

the form of ingots. The ingots were melted in a 60 kg-capacity crucible, using an electrical resistance furnace. The melting temperature was held at 740±5°C. The molten metal was degassed for 15 minutes using pure dry argon injected into the molten metalby means of a graphite rotary degassing impeller. After degassing, the molten metal surface was skimmed carefully to remove all the oxide layers and dross before pouring the melt into the ingot molds. Samplings for chemical analysis were also taken simultaneously for each alloy melt composition prepared-Table 2.The main additives e.g. Sr, Ti, and Zr, were introduced in the form Al-10wt%Sr, Al-5wt%Ti-1%B, Al-25 wt% Zr, master alloys respectively. Silver was added in the form of pure metal (99.99 wt%Ag).

Heat Treatment

The ingots thus prepared were later remelted in the low pressure die casting furnace that was used for preparing the LPDC test bars. The mold cavity was filled by forcing the molten metal (using pressurized gas at 0.3 to 1.5 bar) the molten metal to rise into a ceramic tube which connects the die to the furnace. The tensile test bars were subsequently cut from their castings with dimensions corresponding to ASTM B-108 type dimensions. As for the 319 alloy, the degassed metal was poured into a permanent ASTM B-108 metallic mold preheated at 450°C.

The as-cast tensile test bars were subjected to T6 heat treatment which consisted of (a) solution heat treatment (SHT) at 495°C for 8 hours, followed by (b) quenching in warm water, and then(c) artificial aging either at 160°C and 220°C for times up to 200h(mainly for the 319 alloy), or at temperatures of 155, 180, 200, 220, 240 and 300°C for 5 hours at each temperature (the 220 based alloys). Samples were sectioned from as-cast and heat-treated tensile-tested bars for metallographic examination. The polished samples were examined using an image analyzer system. The volume fraction of intermetallic phases in these samples was determined using an electron microprobe analyzer equipped with EDS and WDS facilities. Grain size measurements were carried out for all the alloys investigated. For these measurements, etched samples were examined using the optical microscope coupled with a Clemex image analyzer system; the linear intercept method was employed to determine the average grain size in each case.

Tensile Testing

All test bars were tested at room using an MTS servohydraulic mechanical testing machine. A data acquisition system attached to the machine provided the tensile test data. The test bars were pulled to fracture at room temperature at a strain rate of 4×10^{-4} s^{-1}. A strain gauge extensometer was attached to the test bar to measure percent elongation as the load was applied. The yield strength (YS) was/calculated according to the standard 0.2% offset strain, and the fracture elongation was calculated as the percent elongation (%El) over the 50 mm gauge length of the test bar. The ultimate tensile strength (UTS) was also obtained from the data acquisition system of the MTS machine. The machine was calibrated each time before any testing was carried out. For each testing condition five test bars were used and the average was plotted.

Metallography

Samples were sectioned for the selected tested tensile bars. These samples were polished following standard method and examined using Clemex image analyser in conjuction with optical microscope. [12].In order to arrive at a better understanding of the role of precipitation of age hardening phase, polished samples from the 220A alloy at different working conditions were examined using a Hitachi SU-8000 field emission scanning electron microscopeequiped with X-ray energy dispersive system (EDS) as well as wavelength dispersion spectroscopic (WDS) facilities. Prior to examination, the polished surface surfaces were cleaned using ion bombardment method.

RESULTS AND DISCUSSIONS

Macro-and Microstructure of as Cast Alloys

The grain refining effect of the different additives is presented in Figure 1(a) for all the 220 alloys studied in the present work. For comparison, samples obtained from tensile test bars produced using traditional permanent mold (same dimension as those used in present study) were also plotted in Figure 1(a). The grain size of 220A alloy produced using low pressure die casting technique (LPDC) is significantly much finer than those obtained from the same alloy produced by gravity technique (GDC).As expected, the addition of Ti and Zr contributed further to grain refining of LPDC alloy series leading to about 85% reduction in the grain size - 220I alloy. In general these results are in good agreement with the results obtained by Nabawy *et al.* [9]. Figure 1(b) presents the porosity percentage revealing that bars prepared by LPDC technique are much sounder than those obtained using the traditional GDC method. Figure 2 demonstrates examples of grain structure obtained from 220A and 220I alloys obtained by both casting methods.

Figure 3 shows examples of the microstructure of the 220A and 220I. In both cases the α-Al dendrites may be clearly observed, outlined by the secondary phases present in the interdendritic regions. Compared to the base alloy whichexhibits elongated dendrites in general, the dendrites in alloy I appear to be more equiaxed or rounded in nature. This is to be expected, since the two alloys respectively contain Ti and Zr which are well known for their grain refining action. In Figure 3 (b), the presence of Al_3Zr particles (arrowed) is noted. Figure 3(c) is a high magnification micrograph of the 220A alloy showing the presences of α-$Al_{15}(Fe,Mn)_3Si_2$ marked (A) and Al_2Cu marked (B) intermetallics in the microstructure. In agreement with the data presented in Figure 1(b), Figure 3(d) shows the microstructure of 220G alloy (corresponding to maximum porosity value) exhibiting large shrinkage cavities due to poor feeding when the test bars were produced applying the GDC technique. Figure 3(e) exhibits the microstructure obtained from the 319 alloy revealing the presence of different phases in the as cast condition whereas Figure 3(f) shows the remaining of undissolved Cu-rich phase after solutionizing at 495°C for 8h.

Besides the effect of the grain refiner additions, it is also important to know the type and amounts of intermetallic and other phases formed in these alloys as a result of these additions, as they will also affect the resultant alloy properties. The additives may interact with each other and with the alloying elements present in the alloy to produce various phases depending on the melt and solidification conditions. Some of these interactions may have a deleterious effect on the resultant properties. For example, the presence of Sr in Al-Si-Cu based alloys is known to create an increase in porosity and also cause segregation of the copper phases in the interdendritic regions so that the phase is much harder to dissolve during solution heat treatment as inferred from the study of Han *et al.* [14]. Figures 4 (a&b) show an example of element distribution in 220I alloy containing Zr, Ti and Ag, whereas Figure 4(c) reveals the main elements in the bright particles observed in the back scattered electron image in (a).

Precipitation during Aging

Figure 5 presents the microstructure of the 220A alloy in the as cast condition. In addition to the aluminum matrix the microstructure reveals the presence of Al_2Cu and α-$Al1_5(Si,Fe)_3Si_2$intermetallics. After solutionizing for 8 hours at 495°C, fine particles of the order of 50nm were observed in the microstructure as exhibited in Figure 5(b). According to Tavitas-Medrano et *al.*[15], these particles could be a mixture of Si and Al_2Cu. It be mentioned here that the samples were kept at 25°C for about 30 days prior to examination. As expected aging at 180°C for 5 hours (corresponding to maximum obtained UTS levels) resulted in dense precipitation of fine Al_2Cu phase particles (30-80 nm) covering the entire matrix as

presented in Figure 5(c). It is evident that there is a distinct difference in the shape and size of the precipitated particles on going from 180°C to 220°C. In the latter, the particles appear in the form of short rods with a relatively larger area of soft aluminum matrix Figure 5(d), compared to that observed in Figure 5(c), which would lead to commence of softening.

A higher magnification electron micrographs obtained at this aging condition is shown in Figure 5(e) where the particle precipitation took place within the aluminum matrix as well as on the pre-existing phases such as Al_7Cu_2Fe as conformed from the associated EDs spectrum shown in Figure 5(f). Increasing the aging temperature to 300°C resulted in complete conversion of the spherical particles shown in Figure 5(c) to rather rod-like particles occurring in two perpendicular directions. Figure 5(h) clearly shows a significant increase in the soft α-Al matrix.

Mechanical Properties

The 319 Alloy

Figure 6 presents the variation in the 319 alloy as a function of aging time at 155°C and 220°C. As expected increasing the aging time at 160°C resulted in continuous increase in the alloy strength reaching about 425MPa after 60h followed by over-aging. At 220°C, the alloy reached peak-aging after only 6h. The broken line in Figure 6(a) represents the 5h aging time used for the other alloys. The alloy apparently achieved UTS values of 370 MPa and 320 MPa at 160°C and 220°C, respectively. Similar trend was exhibited by the YS. Figure 6(b) displays the variation in the alloy % elongation. Maximum obtainable ductility (4%) was produced after aging for 60h at 220°C. Aging for 5h produced only 2.5%. Figure 7 shows the quality index chart for the 319 alloy where the alloy reached the peak-aging point after 40h at 155°C or 12h at 220°C. It should be noted here that 0h corresponds to the SHT condition. As it is inferred from Figure 7, aging the 319 alloy for 6h at 160°C or 220°Cproduces an average Q value of about 375MPa (circled area).

The 220 Alloys

As Cast and Solution Heat Treated Conditions

The UTS values obtained for the 220 alloys studied in the as-cast and solution heat-treated conditions for both series of alloys-Figure 8. The tensile strength values lies in the range of 220 MPa to 250 MPa for LPDC alloys in the as-cast condition. Following solution heat treatment these alloys exhibitevalues in the range of 265-315 MPa for the same alloys after solution heat treatment, with an average overall increase of about 23.4%. The observed increase in tensile strength may be attributed to the dissolution of the Cu-rich intermetallic phase particles, mainly the Al_2Cuphase during solution treatment, and solid solution hardening is the process mainly responsible for the observed increase in strength. The results also show that alloys G and E possess UTS values in the as-cast condition that were lower than that of the base alloy A. This may be attributed to the relatively high volume fraction of intermetallics observed in these alloys. Both these alloys contain 0.15%Ti + 0.50%Zr, with alloy G containing 0.70% Ag in addition.

According to Reich et al. [18]and Rosalie and Bourgeois [19] who investigated the evolution of the Ag rich phase (which is similar in structure to the θ-$CuAl_2$ phase) in Al-Cu-Mg-Ag alloys, several studies are reported in the literature which propose different structures of the Ω phase, and how the addition of Ag changes the precipitation process which normally occurs in Al-Cu-Mg alloys. et al. [20] have reported, however, that while Ag is not needed for the formation of the Ω phase, its presence greatly increases the number density of these precipitates in the alloy. The mechanism by which Ag promotes the nucleation of the Ω phase is still not known as reported in Ref [20].

The improvement in tensile strength of alloy B (containing 0.02%Sr) in comparison to the base alloy may be

attributed to the refining effect of Sr on the morphology of the α-Fe script intermetallic phase, which leads to a more even distribution of the α-Fe phase particles within the matrix [21] Similarly, in the case of grain refining additions, the presence of Ti and Zr, enhances the tensile strength in alloys C and F, due to the decrease in grain size of 320μm in the base alloy A to much lower value of 76 μm. In the as-cast condition, therefore, the best combination for maximizing UTS appears to be 0.15 Ti + 0.30 Zr.The tensile strength values of the 220 alloys are considerably enhanced following solution heat treatment, particularly in the case of alloys B, G and C. In the case of Alloy B, the Cu-rich intermetallic phase is almost completely dissolved in solid solution, so that the volume fraction of these intermetallics in the microstructure is reduced by about a third, asreported by Elgallad [21] who carried out a detailed microstructural investigation of permanent mold cast 220 alloys.

The YS values, which range from 162 to 193 MPa (average 177.5 MPa) in the as-cast samples, increased to 180-205 MPa after solution treatment (average 192.5 MPa), with an overall average increase of ~8.5%. Any mechanism which resists the mobility of dislocations in an alloy will increase its yield (and tensile) strength. The yield strength values of alloy D (and alloy I to a lesser extent) are lower compared to other alloys. This observation may be attributed to the interactions between Sr and Ti, or Sr and B (from the Al-5Ti-1B master alloy used for the Ti additions) which have been reported by Liao et al.[22] and Chenet al.[23]to cause mutual 'poisoning' of the elements. Thus, modificationand/or grain refining effects are suppressed. This is not the case for alloys B and C which contains individual additions of Sr and Ti, respectively. Upon solution heat treatment, the YS values of all alloys increase, in a manner similar to that for the UTS results. The same strengthening mechanisms apply in this case, with solid solution strengthening acting as the operating mechanism.

The percent elongation exhibited by these alloys increased from an average of roughly 2.3% in the as-cast state to values that range from 3.3% to 5.2% after solution treatment, with an overall average of ~4.3%. Compared to this average, alloy C exhibited a relatively higher elongation of 5.8%, which alloy B attains the maximum ductility at 6.8% among all the alloys studied. The dissolution of the Cu-rich intermetallic phases due to the presence of Sr, as well as its effect on refining the α-Fe intermetallic phase so that it is more evenly distributed in the matrix are the reasons for the large increase in the observed elongation.

Effect of Aging Condition

Figures 9 (a-c) show how the tensile properties of the 220 alloys studied vary with aging temperature. Compared to the range of UTS values (Figure 8(a)) exhibited by the solution-treated alloys (265 to 315 MPa), aging at 155°C increases the strength by ~16.6% on average (330 to 352 MPa) over the four groups of alloys studied, the highest improvements being noted for the E, F and G alloys. The addition of Zr-Ti produces a refined non-dendritic structure that decreases the probability for porosity formation.

Additionally, dispersoid precipitates of Al_3Zr and/or $Al_3(Zr_{1-x}Ti_x)$ may act as nucleation sites for the hardening phases during the aging process, resulting in further improvement in strength. These observations are in good agreement with those reported by Yu et al. [24] on the performance of aluminum alloys with Al_3(Sc,Zr) phases, and Qzbilen [25] on the influence of Zr addition on S'-precipitation in an Al-Cu-Mg. In order to enhance the mechanical properties of an aluminum alloy, it is important to obtain a thermally stable microstructure and coarsening-resistant dispersoids. This may be achieved by adding Zr, which has the smallest diffusion flux in aluminum of all the transition metals; the presence of Zr leads to the formation of fine dispersoids that resist coarsening at higher temperatures, which helps to improve/maintain the

mechanical properties as discussed by Mahmudiet al. [26].

In both alloy series peak aging is achieved mainly at 180°C, although in some cases, this may spread up to 200°C. Softening begins as the aging temperature is increased above this range, so that with the coarsening of the precipitates, the alloy strength decreases and a corresponding increase in ductility is observed.

With respect to the alloy yield strength, Figure 9(b) reveals that the base alloy A and alloys B, C and D show almost identical behavior as the aging temperature is increased from 155°C to 300°C. Alloys E, F, G, H and I produced by LPDC technique, also show more or less similar behavior across this range of aging temperatures. At 155°C, the YS value is 250 MPa regardless of the Sr and/or Ti additions of this group. In comparison, the YS values for the other three groups increase by about 20-45 MPa due to the Zr, and Ag additions. The highest YS values are observed within the peak aging temperature range of 180-200°C, with maximum YS values being exhibited by alloys G and I.

It is interesting to note that these alloys contain one or more of the elements Ti, Zr and Ag in different amounts. Alloy 220I, which shows YS values of 346-348 MPa, indicates that a high Zr level (0.5 wt%) greatly improves the yield strength, due to its influence in controlling the evolution of the grain size and the sub-grain structure through the formation of a copious amount of Al_3Zr phase dispersoids. The resistance of these dispersoids to dissolution and coarsening increase the alloy yield strength during precipitation hardening. Similarly, the alloys G, and I give rise to the formation of Al_3(Zr,Ti) precipitates due to the presence of combined Ti+Zr (alloy F), or Ti+Zr+Ag+Sr (alloy I) additions.

In keeping with the tensile strength results shown in Figure 8, the alloy ductility varies accordingly, the lowest ductility values being observed in the peak aging temperature range of 180-200°C (Figure 8(c)). Alloy D shows the lowest ductility values across the aging temperature range, regardless the casting technique, even lower than the base alloy A. This may be attributed to the interaction between Ti and Sr, reducing the benefits of the individual additions. This indicates that the alloy is more resistant to softening than the other alloys. While all alloys show maximum ductility at 300°C, the greatest amount of softening is noted for the C alloy.

To summarize, these results show that, depending on the end application, the aging conditions for 220 type alloys may be selected to provide the best compromise between strength and ductility required for that application, bearing in mind also the economic benefits of the 5 hours aging time used in this work. Increasing the copper content from 2wt% (220A alloy) to 3.5wt% (319 alloy) does not bring significant increase in the alloy strength as inferred from comparing Figures 6 and 9.

Q-Charts

Quality index charts represent a numerical value that defines the quality of aluminum castings. Taking into consideration the equations developed by Drouzy et.al.[26], which is Directly related to the physical phenomena that control the alloy properties and vary independently. And the Quality index equations proposed by Càcereset. al. [28], which is based on the assumption that the materials curves may follow the Holloman equation [29].

It can be observed in Figures 10 (a-c) that the Q values assume a regular decrease as the age hardening temperature is increased; the alloy curves shift from the upper left corner to the bottom right corner. The increase in the aging temperature provides a rapid aging treatment with economic benefits.The noticeable reduction in the strength and Q values of the 220 alloys, upon increasing the aging temperature, is due to the formation of coarser precipitates with lower density in the matrix displaying major inter-particle spacing. These changes facilitate dislocation motion and result in

softening the alloys, thereby decreasing the strength and the Q values of the castings.

The addition of Ti, Sr, Zr, Ag, and Sc to the 220 alloys affects their Q values, as evident in alloys 220B, 220H, and 220I. For example, alloy 220B (Ti-Sr group) yields better Q values than the 220A base alloy; its Q values decrease smoothly with respect to the increases in the aging temperature.The Q values observed ensure that the addition of Ti-Sr and/or Zr gives the same improvement to the quality of the castings as well as its strength. Observed in Figures 9 allloys containing Ti-Sr and Zr-Ti yields the highest Q values, were alloy 220C demonstrated a value of 453 MPa at an aging temperature of 180°C and alloy 220E gave 440 MPa at an aging temperature of 155°C. The improvement observed in the Q values of each alloy can undoubtedly be attributed to the positive effects of adding Zr and/or Ti, for their grain refining action as well as the formation of precipitates of Al_3Zr and/or $Al_3(Zr_{1-x}Ti)$, which act as nucleation sites for the hardening phases during the aging process, resulting in a further improvement in quality. Zirconium is added to increase the strength of aluminum alloys. It has the smallest diffusion flux in aluminum of all the transition metals. Its addition to aluminum base alloys results in the formation of the Al_3Zr phase. These particles are resistant to dissolution and coarsening, and control the evolution of the grain and subgrain structure, thus providing the means to enhance the alloy quality in the precipitation-hardened T6 condition.

Figure11 displays the quality charts obtained for the 220 alloys studied separated into the four groups. These charts were generated using the Caceres approach [28,29]. The quality charts shown in Figure 11 provide several significant properties for each point located in these charts, namely, UTS, elongation to fracture, YS, q and Q, and thus allow for the selection and prediction of the appropriate metallurgical conditions to be applied to a specific alloy to obtain the properties desired for a particular application. In general, most of the alloys show a Q value of 406 MPa or less with some exceptions. As may be seen from Figure 11(a), Alloy C exhibits a Q value that approaches the 522 MPa iso-Q line in the peak aged condition (180°C), while other alloys such as Alloys E, F and G show Q values that approach 472 MPa (Figure 10(b)). Yield strengths in the peak aged condition generally exhibit values higher than 327 MPa, which rapidly drop down to 107 MPa at 300°C. It is interesting to observe that the low ductility values exhibited by Alloy D in Figure 9 (c) lower the alloy quality as well so that its curve is shifted further to the left compared to the other alloys.

CONCLUSIONS

The present study was carried out to investigate the effects of Sr, Ti, Zr and Ag additions, individually or in combination, on the performance of an Al-2%Cu based alloy. Using different combinations/amounts of these additives, several alloys were prepared (base alloy A and alloys B through I). Two different techniques were applied to produce samples used in the present work. From the microstructural observations and a tensile test data and quality charts constructed from the latter, the following conclusions may be drawn.

- With the exception of the Cu-rich $CuAl_2$ phase, most of these intermetallics do not dissolve upon solution heat treatment.
- The addition of 0.15%Ti + 0.30%Zr is found to be very effective in refining the grain size,. Increasing the Zr level to 0.50 wt% does not improve upon the refining.
- Alloys containing 0.0 wt%, 0.27 wt% Zr and 0.37wt%Zrshow maximum improvement in the alloy strength.

- The alloy ductility increases from ~2.3% to ~4.3% after solution heat treatment, with alloy B (0.02%Sr addition) exhibiting an elongation of 6.8%.
- The yield strength of Zr free alloys show identical behavior over the range of aging temperatures studied, indicating that the base alloy is not affected by Sr, Ti or Sr+Ti additions.
- Alloy containing 0.35 wt% Zr + 0.55 wt%Ag exhibits maximum YS (346-348 MPa), showing that a high addition of Zr (0.50%), resulting in a profuse formation of Al_3Zr precipitates, greatly improves the yield strength.
- Quality charts constructed from tensile properties data may be used for the selection of the appropriate metallurgical conditions for tailoring the alloy properties to those required for a specific application.
- Increasing the copper content from 2wt% to 3.5 wt% does not produce significant increase in the alloy strength.

ACKNOWLEDGEMENTS

The authors would like to thank Ms Amal Samuel for enhancing the image quality in the presentpaper.

REFERENCES

1. *Y.L. Chu, P.S. Cheng and R. Shivpuri, Soldering Phenomenon in Aluminum Die Casting: Possible Causes and Cures. NADCA Transactions, Paper No. T93–124, 1993, pp. 361-371.*
2. *M.M. Makhlouf, D. Apelian and L. Wang, Microstructure and Properties of Aluminum Die Casting Alloys. NADCA Transactions, Paper No. DOE/ID/13320-2, 1998, pp. 116-132.*
3. *A.C. Street, The Die Casting Book, 2nd Ed., Red Hill, England, 1990, pp. 611-658.*
4. *E.M. Elgallad, F.H. Samuel, A.M. Samuel and H.W. Doty, Development of new Al-Cu based alloys aimed at improving the machinability of automotive castings. Int. J. Metalcasting, 3(2009), pp. 29-41.*
5. *Y. Yi-Cong, H. Liang-Ju and L. Pei-Jie, Differences of Grain-Refining Effect of Sc and Ti additions in Aluminum by Empirical Electron Theory Analysis, Trans Nonferrous Metals Soc China, 20(2010), pp. 465-470.*
6. *E. Samuel, B. Golbahar, A.M. Samuel, H.W. Doty, S. Valtierra and F.H. Samuel, Effect of grain refiner on the tensile and impact properties of Al-Si-Mg cast alloys. Materials and Design. 56(2014), pp. 468-479.*
7. *P.N. Crepeau, Effect of Iron in Al-Si Casting Alloys: A Critical Review, AFS Trans., 110(1995), pp. 361-366.*
8. *A.M. Nabawy, A.M. Samuel, F.H. Samuel and H.W. Doty, Effects of grain refiner additions (Zr, Ti-B) and of mould variables on hot tearing susceptibility of recently developed Al-2 wt-%Cu alloy. International Journal of Cast Metals Research, 2013.* ***26****(5): p. 308-317.*
9. *A.M. Nabawy, A.M. Samuel, F.H. Samuel and H.W. Doty, Influence of additions of Zr, Ti-B, Sr, and Si as well as of mold temperature on the hot-tearing susceptibility of an experimental Al-2% Cu-1% Si alloy. Journal of Materials Science, 2012.* ***47****(9): p. 4146-4158.*
10. *S. G. Irizalp and N. Saklakoglu,Effect of Fe-rich intermetallics on the microstructure and mechanical properties of thixoformed A380 aluminum alloy, Int. J. of Eng. Sci. and Technol,Vol.17(2014),pp. 58–62.*
11. *G. Pucella, A.M. Samuel, F.H. Samuel, H.W. Doty and S. Valtierra, Sludge formation in Sr-modified Al-11.5 wt% Si diecasting alloys. AFS Trans., 1999, pp. 117-125.*

12. *Nabawy, M., A.M. Samuel, F.H. Samuel and H.W. Doty, Investigation of Chemical Additives on the Microstructure and Tensile Properties of Al-2wt%Cu Based Alloys. Transactions of the American Foundrymen's Society, 2011, p. 119.*

13. *M.F. Ibrahim, E.Samuel, A.M. Samuel, A.M.A. Al-Ahmari and F.H. Samuel, Metallurgical parameters controlling the microstructure and hardness of Al-Si-Cu-Mg base alloys. Materials and Design, 2011.* ***32****(4): p. 2130-2142.*

14. *Y. Han, Y., A.M. Samuel, H.W. Doty, S. Valtierra and F.H. Samuel, Optimizing thetensile properties of Al–Si–Cu–Mg 319-type alloys: Role of solution heat treatment. Materials and Design, 58(2014), pp. 426-438.*

15. *F.J. Tavitas-Medrano, A.M.A. Mohamed, J.E. Gruzleski, F.H. Samuel and H.W. Doty, Precipitation-hardening in cast AL-Si-Cu-Mg alloys. Journal of Materials Science, 2010.* ***45****(3): p. 641-651.*

16. *M. Voncina, A. Smolet, J. Medved,P.Mrvar, and R. Barbic, Determination of precipitation sequence in Al-alloys using DSC method, Materials and Geoenvironment, 57 (2010) pp. 295–304.*

17. *D.G. Eskin, Decomposition of Supersaturated Solid Solution in Al-Cu-Mg-Si Alloys. J. Mater. Sci., 38(2003), pp. 279-290.*

18. *L. Reich, M. Murayama and K. Hono, Evolution of Ω Phase in an Al-Cu-Mg-Ag Alloy-A Three-Dimensional Atom Probe Study. ActaMaterialia, 46(1998), pp. 6053-6062.*

19. *J.M.Rosalie and L.Bourgeois," θ′ Silver segregation to(Al2Cu)-Al interfaces in Al-Cu-Ag alloys,philos.Mag.89(2009), pp.2195-2211.*

20. *A. Garg, Y.C. Chang and J.M. Howe, Precipitation of the Omega Phase in an Al-4.0% Cu-0.5%Mg Alloy. ScriptaMetallugicaetMaterialia, 24(1990), pp. 677-680.*

21. *E.M. Elgallad, Effect of Additives on the Mechanical Properties and Machinability of a New Aluminum-Copper Base Alloy, Ph.D. Thesis, UQAC, Quebec, Canada, 2010.*

22. *H. Liao, Y. Sun and G. Sun, Effect of Al-5Ti-1B on the microstructure of Near-Eutectic Al-13%Si Alloys Modified with Sr. J. Mater. Sci., 37(2002), pp. 3489-3495.*

23. *C.L. Chen, A. Richter and R.C. Thomson, Mechanical Properties of Intermetallic Phases in Multi-Component Al-Si Alloys Using Nano-indentation, Intermetallics, 17(2009), pp. 634-641.*

24. *K. Yu, W. Li, S. Li and J. Zhao, Mechanical Properties and Microstructure of Aluminum Alloy2618 with Al_3(Sc,Zr) Phases. Mater. Sci. Eng., A368 (2004), pp. 88-93.*

25. *S. Qzbilen and H.M. Flower, Zirconium-Vacancy Binding and Its Influence on S'-Precipitation in an Al-Cu-Mg Alloy. ActaMetallurgica, 37(1989), pp. 2993-3000.*

26. *R. Mahmudi, P. Sepehrband and H.M. Ghasemi, Improved properties of A319 aluminum casting alloy modified with Zr. Materials Letters, 60(2006), pp. 2606-2610.*

27. *M. Drouzy, S. Jacob and M. Richard, "Interpretation of Tensile Results by Means of Quality Index and Probable Yield Strength," AFS International Cast Metals Journal, 5(1980), pp. 43-50.*

28. *C.H. Cáceres, M. Makhlouf, D Apelian, and L Wang,Quality index chart for different alloys and temperatures: a case study on aluminium die-casting alloys, Journal of Light Metals,1(2001), pp. 51–59.*

29. *J. Hernandez-Sandoval, G.H. Garza-Elizondo, A.M. Samuel, S. Valtiierra and F.H. Samuel, The ambient and high temperature deformation behavior of Al–Si–Cu–Mg alloy with minor Ti, Zr, Ni additions.Materials & Design, 58 (2014) pp.89-101.*

APPENDICES

List of Tables

Table 1: Chemical Composition (wt%) of the Base Alloys

Alloy Code	Cu	Si	Mg	Fe	Mn	Sr	Ti	Calculated density (g/cm^3)
220A	2.28	1.28	0.36	0.39	0.61	0.00	0.04	2.78
319(BS)	3.58	6.75	0.29	0.30	0.25	000	0.04	2.93

Table 2: Chemical Composition (wt%) of the Alloys Investigated in the Current Study

Alloy Code	Cu	Si	Mg	Fe	Mn	Sr	Ti	Zr	Ag
220B	2.35	1.21	0.35	0.40	0.60	0.02	0.07	0.00	0.00
220C	2.36	1.13	0.35	0.39	0.60	0.00	0.23	0.00	0.00
220D	1.87	0.98	0.23	0.53	0.53	0.017	0.19	0.00	0.00
220E	2.32	1.16	0.34	0.40	0.62	0.00	0.14	0.36	0.00
220F	2.32	1.12	0.37	0.36	0.59	0.00	0.21	0.27	0.00
220G	2.29	1.09	0.33	0.37	0.57	0.00	0.21	0.36	0.51
220H	1.91	1.00	0.32	0.56	0.56	0.015	0.12	0.65	0.00
220I	1.91	1.00	0.31	0.54	0.54	0.016	0.18	0.35	0.55

Table 3: Total Volume Fraction of Intermetallics Observed in the Present Alloys

Alloy	A	B	C	D	E
Average	3.98	3.91	3.69	2.91	5.74
Std Dev.	0.42	0.44	0.02	0.31	0.9
Alloy	**F**	**G**	**H**	**I**	
Average	4.87	3.88	5.17	3.89	
Std Dev.	0.65	0.45	0.59	1.04	

List of Figures

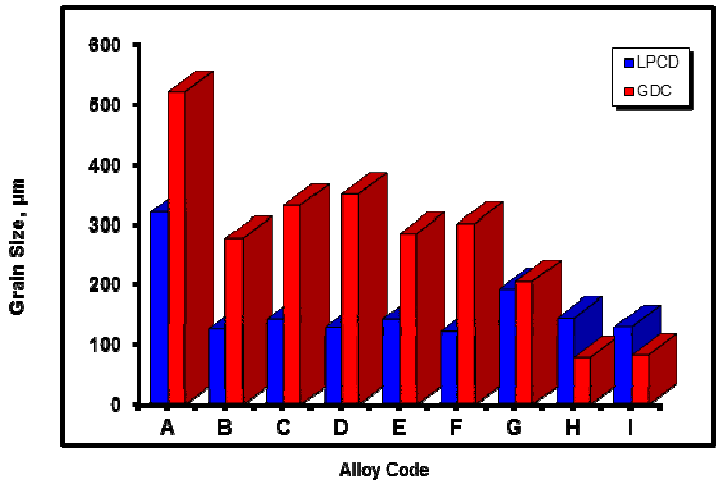

Figure 1(a): Grain Size Measurements Obtained from Both GDC and LPDC Samples

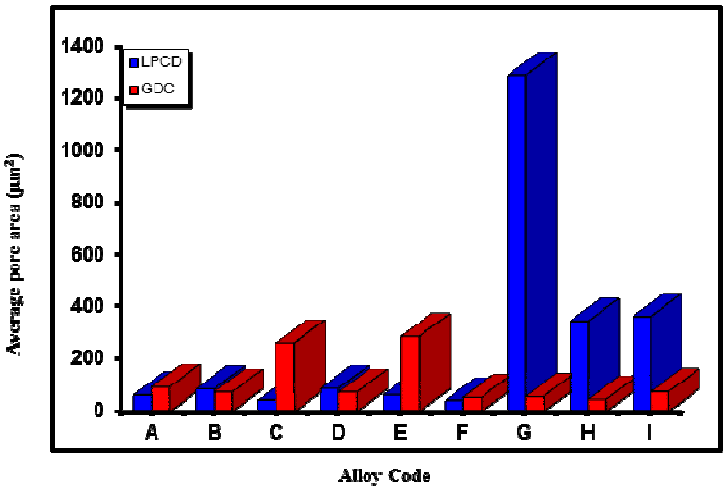

Figure 1(b): Comparison of Area Percent Porosity Produced by LPDC and GDC Processes

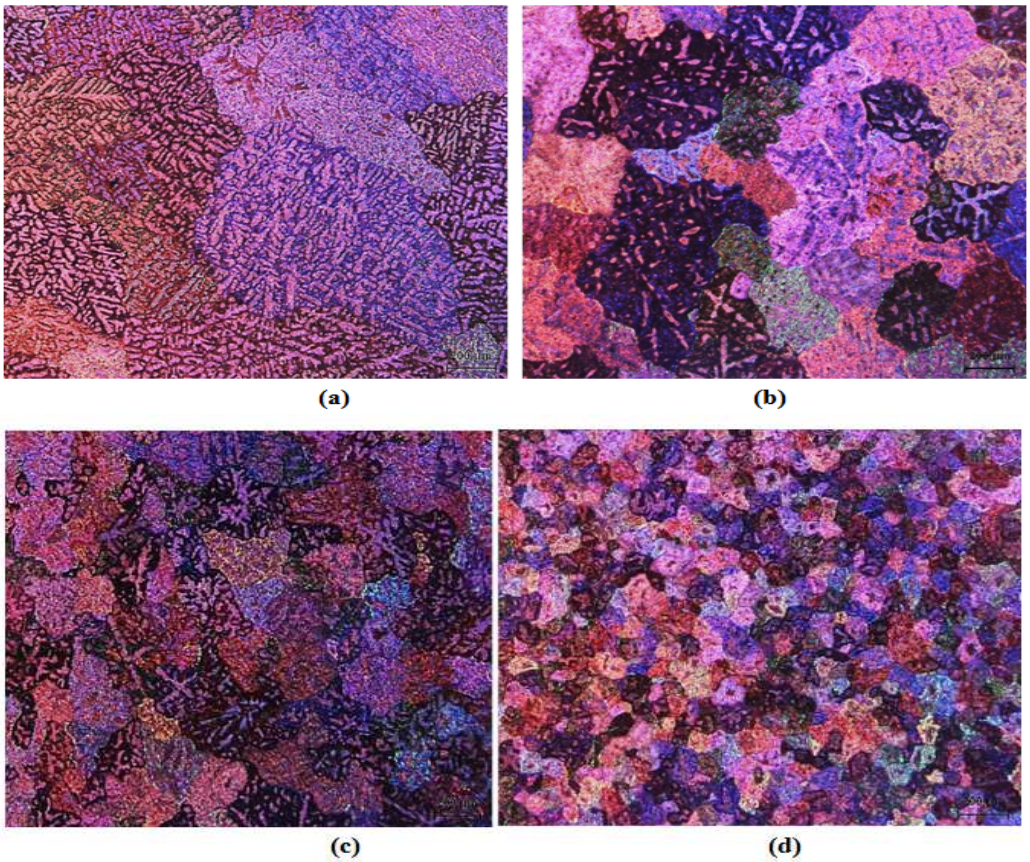

Figure 2: Macrostructure of Etched Samples Obtained From:
(A) 220A-GDC, (B) 220I-GDC, (C) 220A-LPDC, and (D) 220I-LPDC

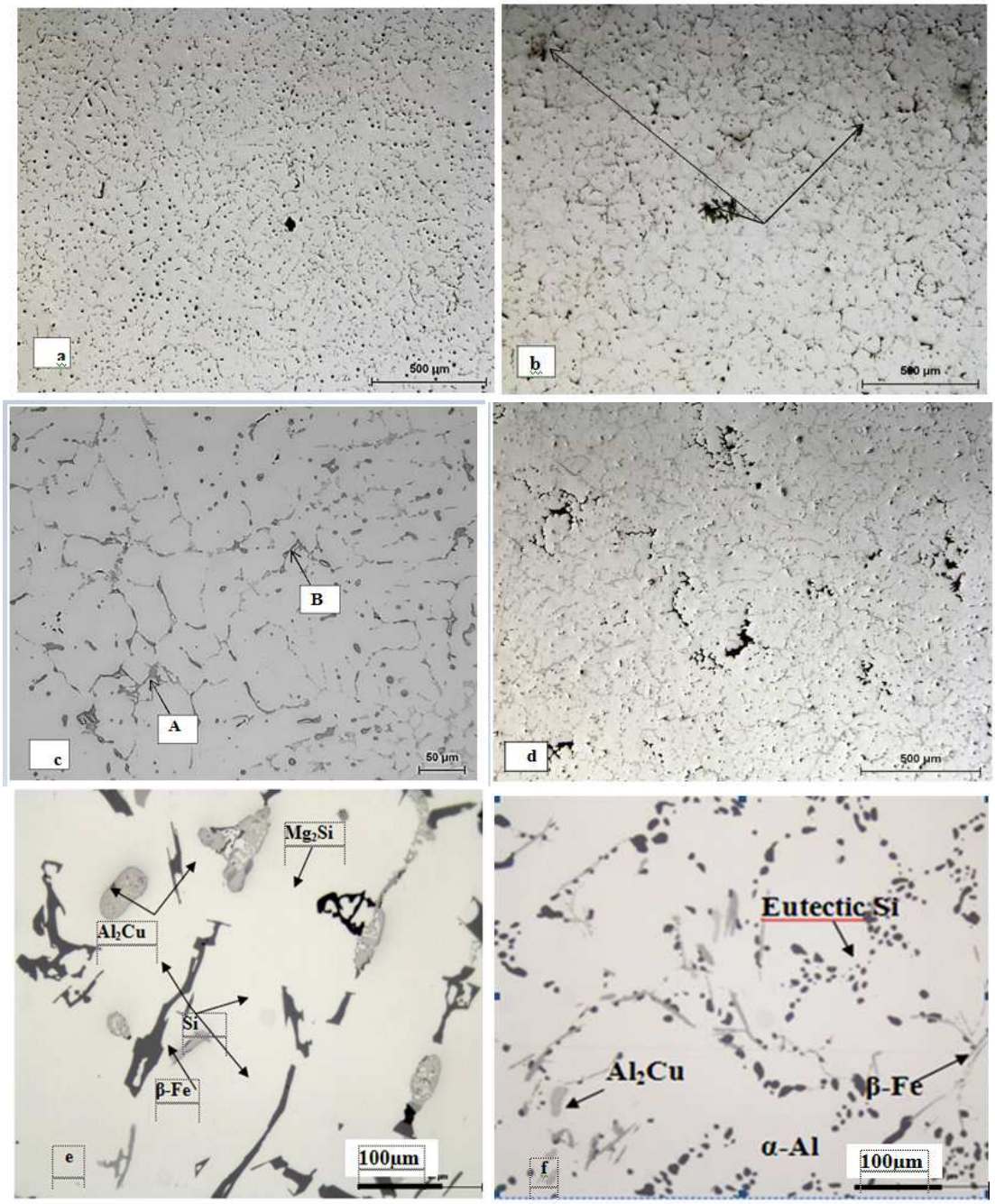

Figure 3: Microstructures Obtained from Samples in the as Cast Condition: (a) 220A-LPDC, (b) 220I-LPDC, and (c) A High Magnification of (a), (d) 220G alloy-GDC, (e) 319 Alloy-as Cast, (f) 319 Alloy-SHT Condition

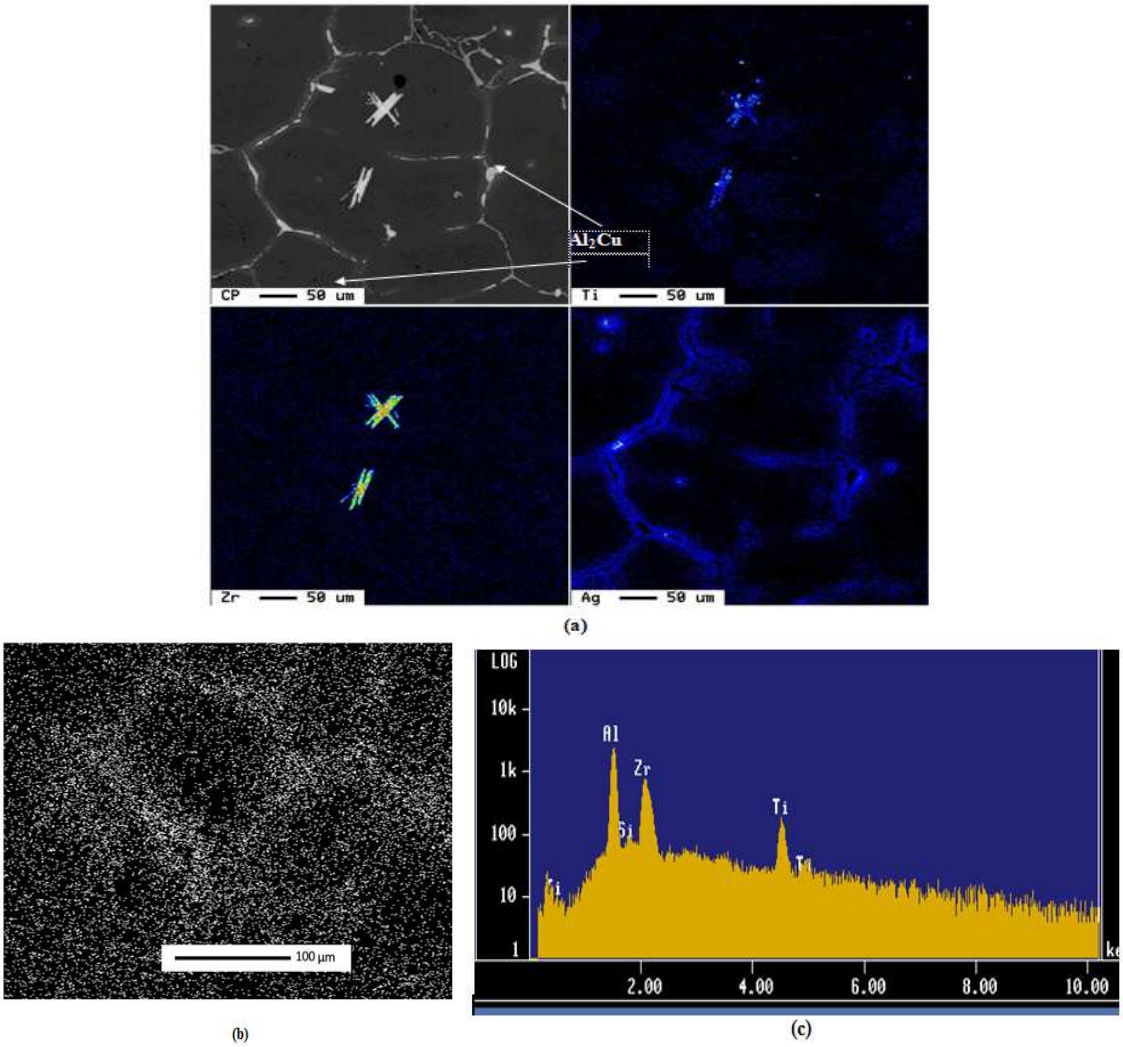

Figure 4: Distribution of Zr, Ti, and Ag in 220I Alloy-LPDC:(a) Element Distribution, (b) Cu Distribution, (c)EDS Spectrum Corresponding the Bright Particles in (a-CP)

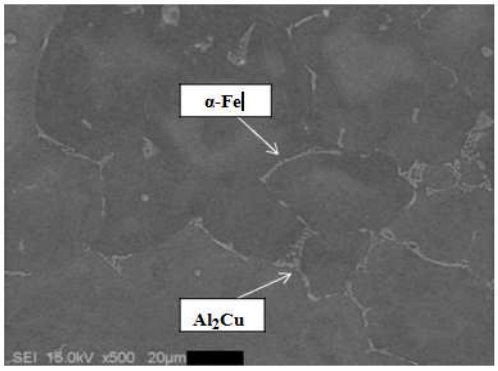

Figure 5(a):Secondary Electron Micrograph of 220A Alloy in the as Cast Condition

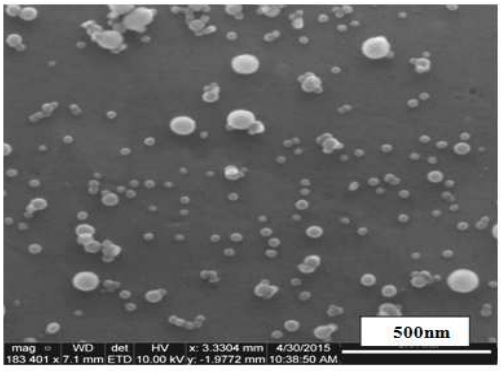

Figure 5(b):Secondary Electron Micrograph of 220A Alloy followingSolutionizingat 490C for8h Followed by Quenching

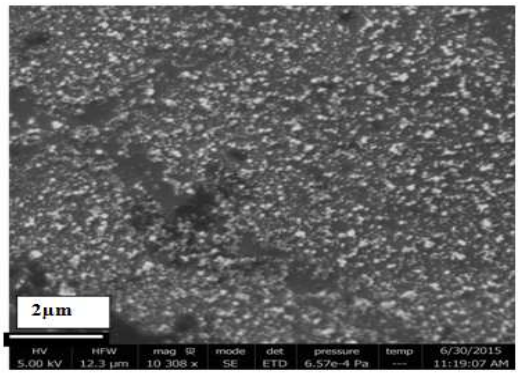

Figure 5(c):Secondary Electron Micrograph of 220A Alloy Aged at 180°C for 5h

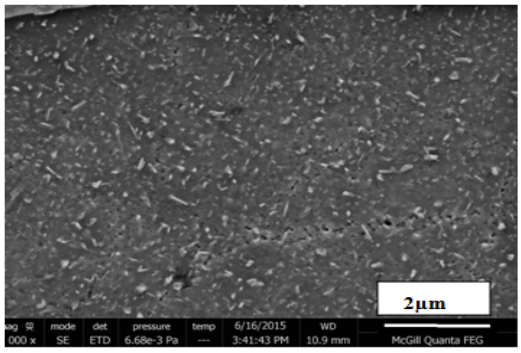

Figure 5(d):Secondary Electron Micrograph of 220A Aged at 220°C for 5h

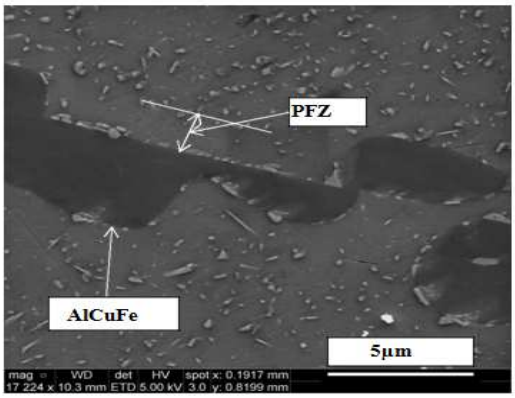

Figure 5(e):A High Magnification Electron Micrograph of 220A Aged at 220°C for 5h.

Note thePresence of Precipitate Free Zones around the Pre-Existing Phase Particles

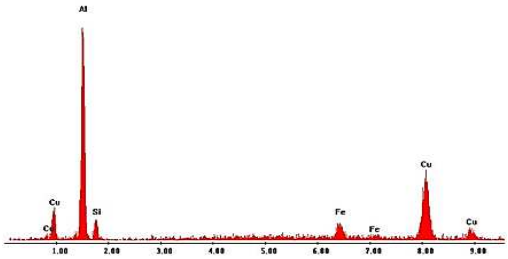

Figure 5(f):EDS Spectrum Corresponding to (e) Revealing Explicit Peaks Due to Al, Fe, and Cuelements

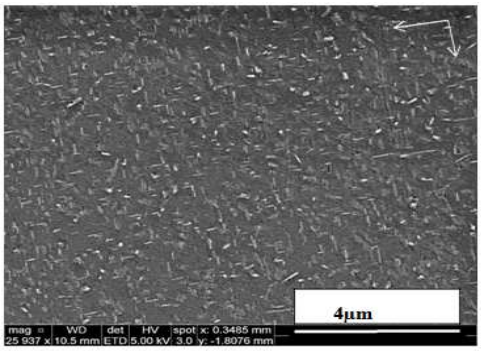

Figure 5(g):Secondary Electron Micrograph of 220A Aged at 300°C for 5h

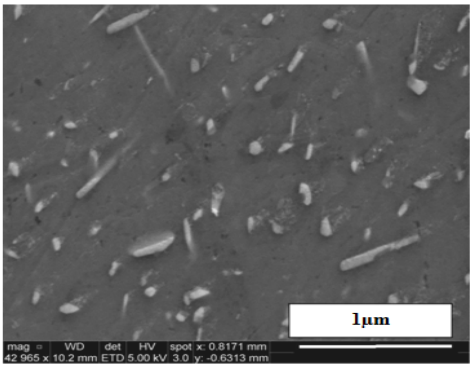

Figure 5(h):A High Magnification Electron Micrograph of 220A Aged at 300°C for 5h

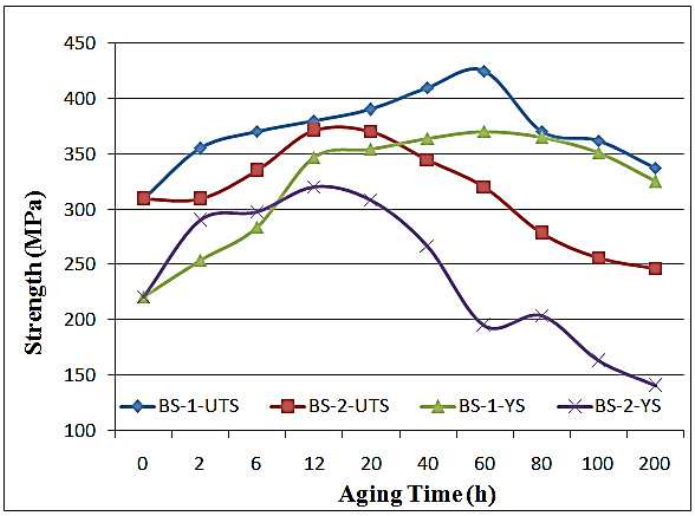

(a)

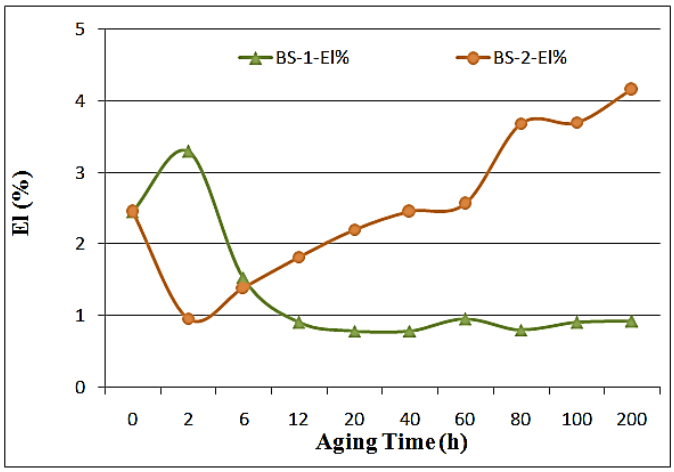

(b)

Figure 6: Variation of the Tensile Properties of 319 Alloy as Function of Aging Condition: (a) Strength, (b) % Elongation.BS-1,155°C, BS-2, 220°C. The zero Time Corresponds to SHT Condition and Broken Lines Represent the 5h Aging Time

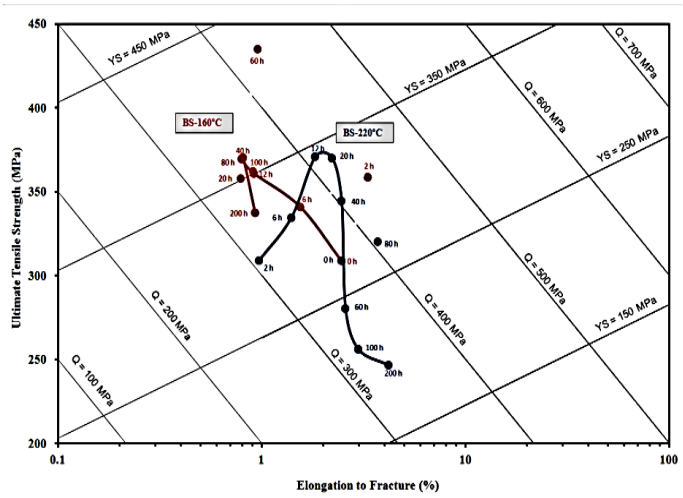

Figure 7: Qulality Index Chart of 319 Alloy in the Aged Condition [Xx]

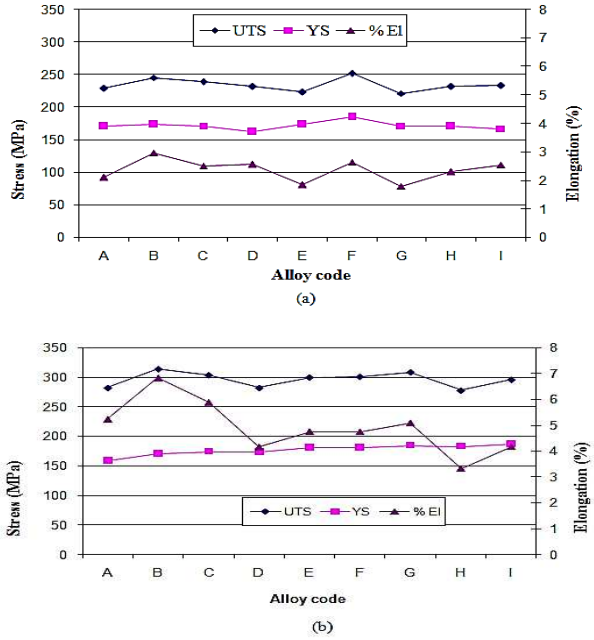

Figure 8: Vartiation in the Tensile Properties of the 220 Alloys in the: (A) as Cast, (B) Sht Conditions

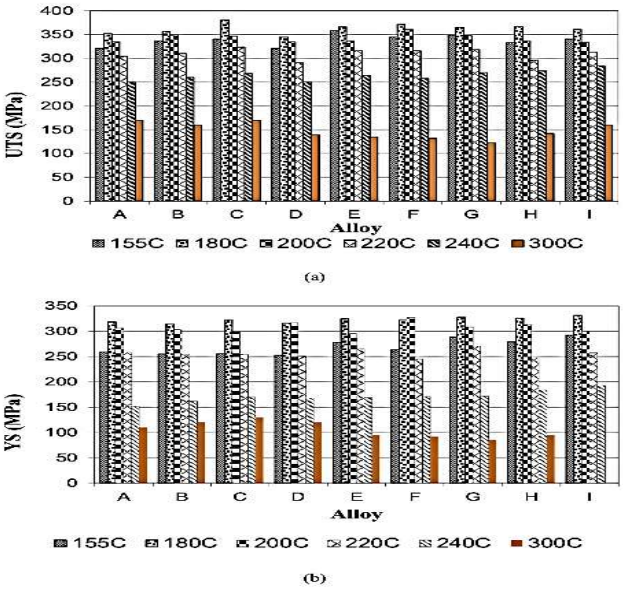

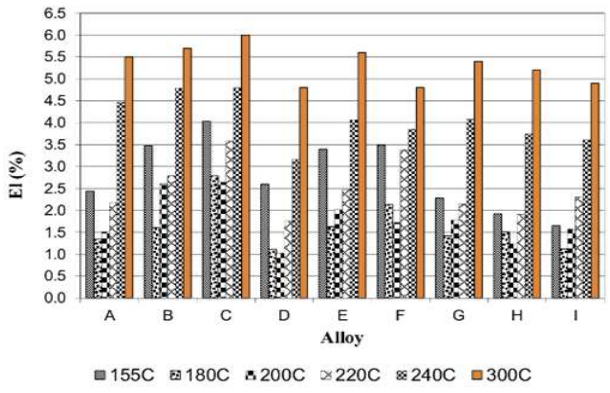

(c)

Figure 9: Tensile Values Obtained from LPDC Samples following T6 Treatment: (a) UTS, (b) YS, and (c) %EI

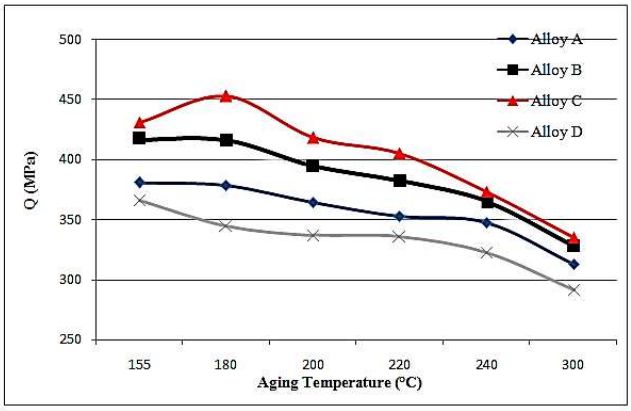

(a)

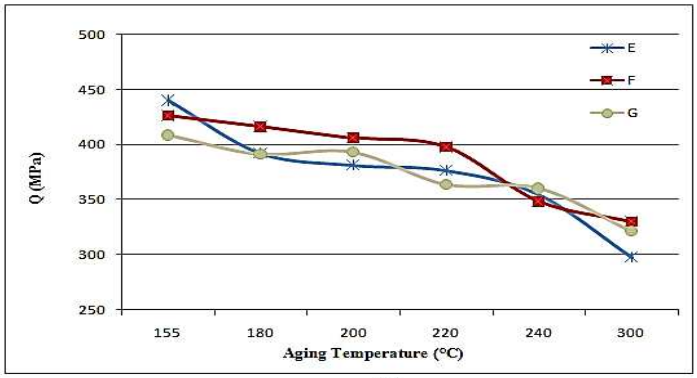

(b)

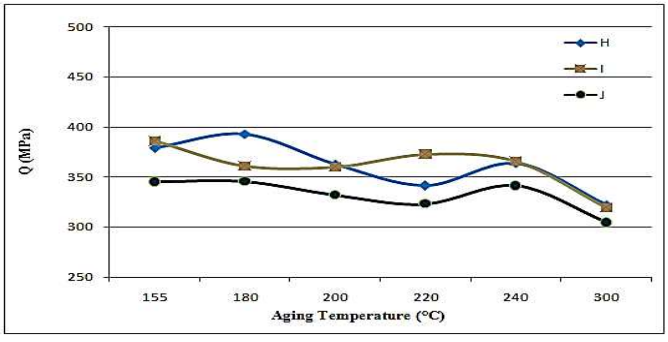

(c)

Figure10: Variation in theQuality Index Values for 220 Alloys as a Function of Aging Temperature (Using the EquationDeveloped by Drouzyet.al[27])

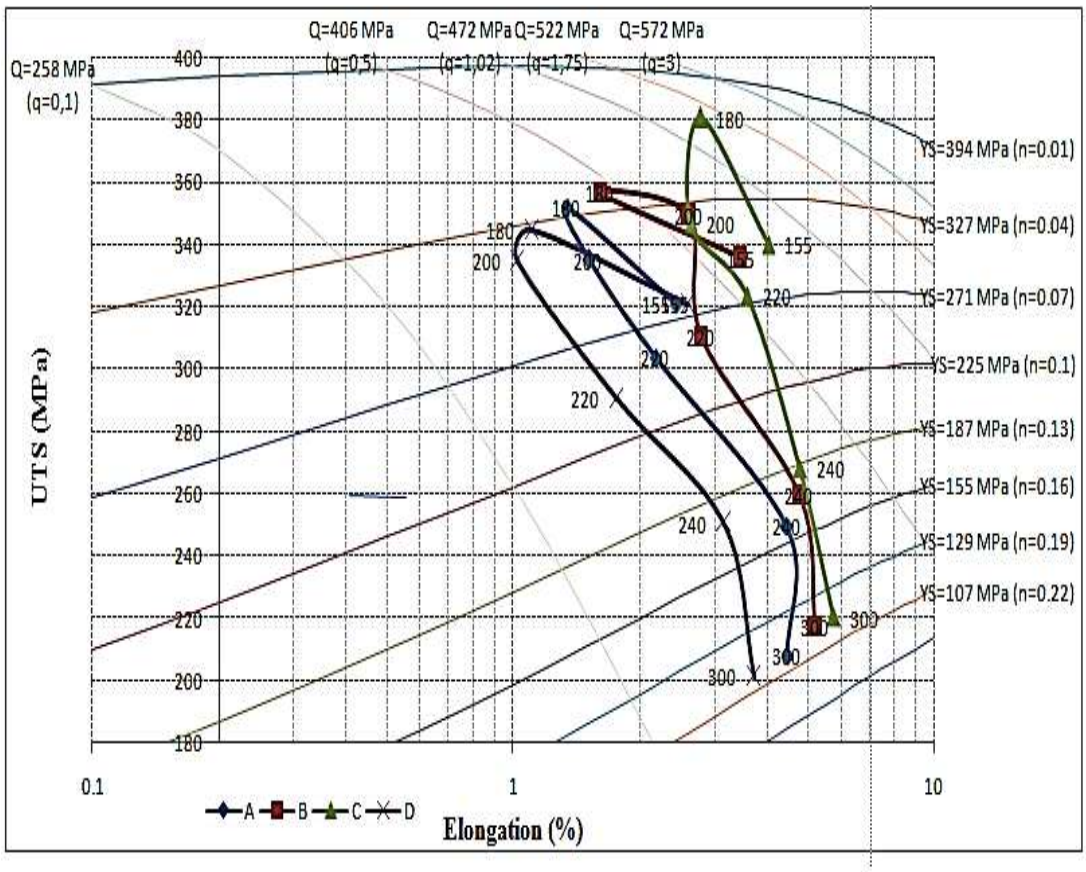

(a)

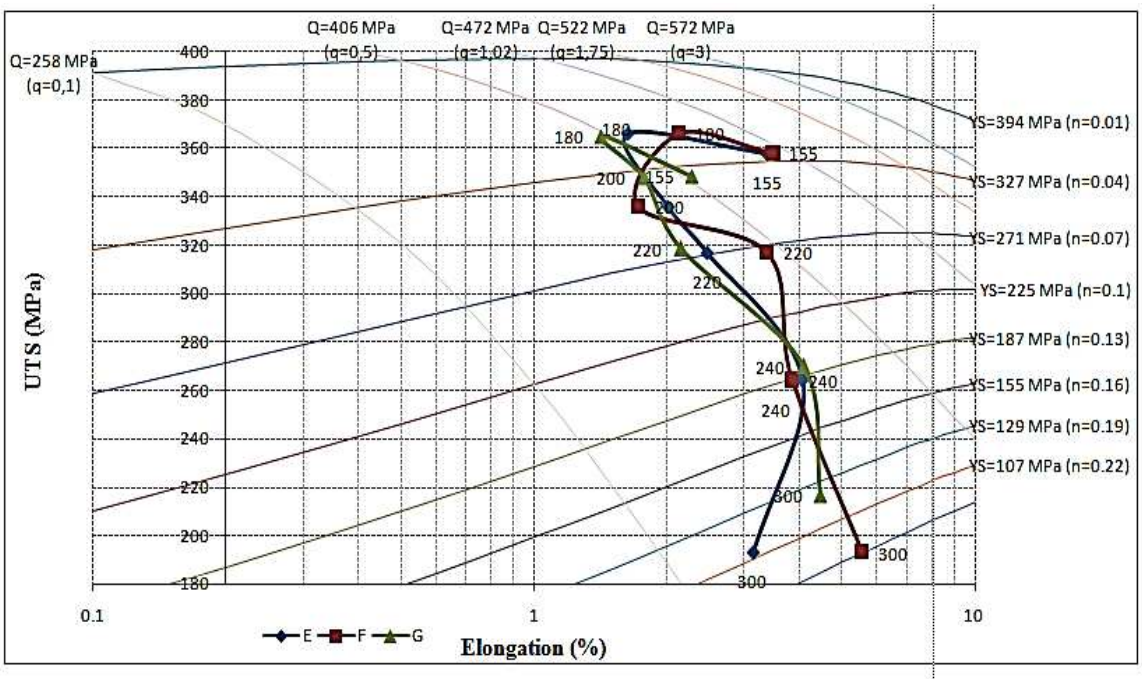

(b)

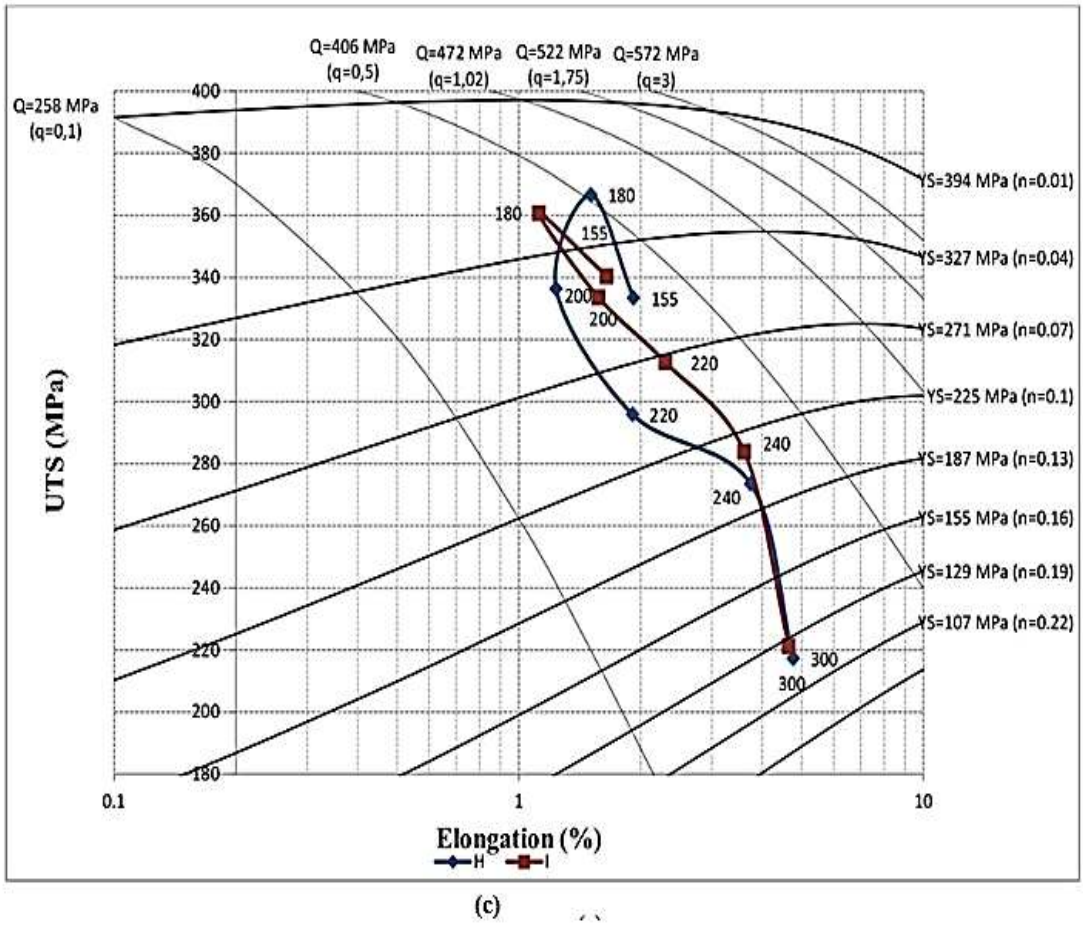

Figure11: Quality Charts of the 220 Alloys in the Aged Condition Following Càceres[28]: (a) 220A,220B, 220C, 220D Alloys, (b)220E,220F,220G Alloys, (c) 220H, 220I Alloys